

1 Ice stream activity scaled to ice sheet volume during Laurentide 2 Ice Sheet deglaciation

3
4 C. R. Stokes¹, M. Margold^{1†}, C.D. Clark², L. Tarasov³

5 ¹*Department of Geography, Durham University, Durham, UK*

6 ²*Department of Geography, University of Sheffield, Sheffield, UK*

7 ³*Department of Physics and Physical Oceanography, Memorial University, St John's, Canada*

8 *Correspondence to: c.r.stokes@durham.ac.uk

9 †Present address: *Department of Physical Geography, Stockholm University, Sweden*

10
11
12 **The sea-level contribution of the Greenland and West Antarctic ice sheets has**
13 **accelerated in recent decades, largely due to the thinning and retreat of outlet glaciers**
14 **and ice streams¹⁻⁴. This ‘dynamic’ loss is a serious concern, with some modelling studies**
15 **suggesting that a major ice sheet collapse may be imminent^{5,6} or potentially underway in**
16 **West Antarctica⁷, but others predicting a more limited response⁸. A major problem is**
17 **that observations used to initialise and calibrate modelling typically span just a few**
18 **decades and, at the ice-sheet scale, it is unclear how the entire drainage network of ice**
19 **streams evolves over longer time-scales. This represents one of the largest sources of**
20 **uncertainty when predicting ice sheet contributions to sea level rise⁸⁻¹⁰. A key question is**
21 **whether ice streams might increase and sustain rates of mass loss over centuries or**
22 **millennia, beyond those expected for a given ocean-climate forcing⁵⁻¹⁰. Here we**
23 **reconstruct the activity of 117 ice streams that operated at various times during**
24 **deglaciation of the Laurentide Ice Sheet (~22,000 to ~7,000 years ago) and show that**
25 **while they switched on and off in different locations, their overall number decreased,**

26 **they occupied a progressively smaller percentage of the ice sheet perimeter, and their**
27 **total discharge decreased. Underlying geology and topography clearly influenced ice**
28 **stream activity, but - at the ice sheet scale - their drainage network adjusted and was**
29 **linked to changes in ice sheet volume. It is unclear whether these findings are directly**
30 **translatable to modern ice sheets but, contrary to the view that sees ice streams as**
31 **unstable entities that can draw-down large sectors of an ice sheet and accelerate its**
32 **demise, we conclude that they reduced in effectiveness during deglaciation of the**
33 **Laurentide Ice Sheet.**

34 Continental ice sheets are drained by a network of rapidly-flowing ice streams with
35 tributaries of intermediate velocity that extend far into their interiors¹¹. Towards the margins
36 of modern ice sheets, many ice streams become confined within glacial troughs and are
37 referred to as marine-terminating outlet glaciers, whereas others occupy regions of more
38 subdued relief¹². Their large size (1-10s km wide, 10-100s km long) and high velocity (100s-
39 1000s m a⁻¹) means they are an important mechanism through which ice is transferred to the
40 ocean, and thereby impacts on sea level. In contrast to climatically-forced melting¹³, ice-
41 stream dynamics could introduce considerable non-linearity in the response of ice sheets to
42 external forcing⁵⁻⁷. This is viewed as the major source of uncertainty in assessments of future
43 changes in ice sheets and sea level^{1,6,8-10}. Does the drainage network of ice streams arise in
44 response to climatically-driven changes in ice sheet volume, or can it evolve to drive changes
45 beyond that which might be expected from climatic forcing alone?

46 Building on a recent inventory¹⁴ of 117 palaeo-ice streams in the North American
47 Laurentide Ice Sheet (LIS, including the Innuitian Ice Sheet, but excluding the Cordilleran
48 Ice Sheet) ([Extended Data Figure 1](#)), we use the best-available ice margin chronology (based
49 on ~4,000 dates: [Extended Data Figure 2](#))¹⁵ to ascertain the timing of their activity during
50 deglaciation (see Methods). Using the mapped extent of ice streams, we calculated the

51 number operating through time and the percentage of the ice sheet perimeter that was
52 streaming. We also explore their potential ice discharge during deglaciation, albeit with larger
53 uncertainties, which we compare with output from numerical modelling of the ice sheet
54 during deglaciation^{16,17} (see Methods).

55 When the LIS was at its maximum extent ~22 thousand years ago (kyr), ice streams
56 formed a drainage network resembling the velocity pattern of modern-day ice sheets (Fig. 1a,
57 b). Early during deglaciation, numerous ice streams were located in major topographic
58 troughs and drained the marine-based sectors of the northern and eastern margins of the ice
59 sheet for several thousand years (Fig. 1b, c). Ice streaming along the land-terminating
60 margins was more transient and we find that numerous ice streams switched on and off in
61 different locations during retreat. This first empirical assessment of the duration of a large
62 population of ice streams reveals that whilst some ice streams persisted for 5-10 kyr, ~40%
63 operated for <2 kyr, with many (~23%) operating for <0.5 kyr (Fig. 2).

64 Although ice streams activated and deactivated in different locations, we find no
65 evidence for any episodes when the number of ice streams increased substantially (Fig. 3a).
66 From ~22 to ~15.5 kyr, the number of ice streams totalled ~50, but thereafter dropped rapidly
67 (e.g. at ~13 kyr and 11.5 kyr), with <10 ice streams operating after ~11.5 kyr. When
68 normalised by ice sheet volume their number is remarkably stable (Fig. 3b), with ~2 ice
69 streams per 1,000,000 km³ of ice sheet volume for almost 10 kyr. LIS collapse into Hudson
70 Bay after 8.5 kyr triggered a final flurry of ice stream activity, but in a very small ice sheet.

71 At its maximum extent, ~27% of the LIS margin was streaming (Fig. 3c), which is
72 very similar to that found for present-day Antarctica (Fig. 1a). This value decreased to
73 between 25% and 20% from 16 to 13 kyr, but then rapidly drops to ~5% at ~11 kyr.
74 Similarly, our order-of-magnitude estimates of palaeo-ice stream discharge show no obvious
75 increases during deglaciation (Fig. 3d). Rather, this ‘dynamic’ component of mass loss was

76 relatively stable from ~22 to 15 kyr (i.e. $\sim 1,500 \text{ km}^3 \text{ a}^{-1}$), but then rapidly decreased to <400
77 $\text{km}^3 \text{ a}^{-1}$ after 11 kyr, and was <100 $\text{km}^3 \text{ a}^{-1}$ after 9 kyr. When normalised by ice sheet volume,
78 the proportion of dynamic mass loss was relatively stable from 22 to 15 kyr, but then dropped
79 at 13 kyr (Fig. 3e), before increasing temporarily as the ice sheet collapsed around Hudson
80 Bay. A comparison with estimates of total ice stream discharge from a previously-published
81 numerical model of the North American Ice Sheet complex¹⁶ and inferences from surface
82 mass balance modelling at specific time-steps¹⁷, indicates that model-derived Laurentide ice
83 stream discharges are typically higher and more variable (Fig. 3f). Nevertheless, an important
84 conclusion is that both empirical and modelled estimates show a decrease in ice stream
85 discharge from around 15 kyr. Moreover, we find a clear link between ice sheet volume and
86 both the number of ice streams and the percentage of the ice sheet perimeter they occupied
87 (Fig. 4a, b). A similar scaling is seen in both modelled and empirically-derived discharge
88 (Fig. 4c), but we acknowledge there are much larger uncertainties in our estimates of palaeo-
89 ice stream discharge. The relative impact of ice streaming is seen more clearly by plotting ice
90 sheet volume against the total ice stream discharge normalised by the ice sheet volume (Fig.
91 4d), indicating that the relative role of mass loss from streaming was unlikely to have
92 increased as the ice volume decreased during deglaciation.

93 There are a number of factors that influence where ice streams develop, with previous
94 work highlighting their strong association with topographic troughs, calving margins and soft
95 sedimentary beds^{10,18,19}. We note that topography exerted a strong control on ice stream
96 location in the LIS, particularly during early deglaciation (22 to 14 kyr) when its flow was
97 steered by the major marine channels of the Canadian Arctic Archipelago and the high relief
98 coasts along the eastern margin. There is no glacial geomorphological evidence¹⁴ that these
99 ice streams continued to operate once the ice sheet lost its marine margin and retreated onto

100 lower relief terrain. Thus, topographic troughs and the marine margin clearly modulated the
101 number of ice streams operating through time (Fig. 1; Fig. 3a).

102 Elsewhere, ice streams were abundant on low-relief areas that were underlain by soft
103 sedimentary bedrock and thick sequences of till. This includes the western and southern
104 margins of the ice sheet^{14,19,20}, where numerous ice streams switched on and off during
105 deglaciation, with marked changes in trajectory²⁰ (Fig. 1). These networks of sinuous ice
106 streams deactivated as the ice margin withdrew onto the harder igneous and metamorphic
107 rocks of the Canadian Shield, pointing to a geological control that explains the marked
108 reduction in ice stream numbers after ~12 ka (Fig. 3a; Extended Data Figure 3). It is
109 important to note, however, that ice streams continued to activate over the low-relief
110 crystalline bedrock of the Canadian Shield, with several large, wide (100-200 km) ice streams
111 operating for very short periods (few hundred years) during the final stages of deglaciation
112 (after ~10 kyr: Fig. 1d; Extended Data Fig. 3)^{10,21}.

113 Although topography and underlying geology exerted an important influence on ice
114 stream activity, we find no evidence for major ice sheet instabilities linked to ice stream
115 activity that is reflected in the spatial re-organisation of their drainage network (e.g. marked
116 increases in the number of ice streams or individual ice streams widening/enlarging during
117 ice sheet retreat). Rather, we find that their overall number decreased and they occupied a
118 progressively smaller percentage of the ice sheet perimeter. This implies that the final 4-5 kyr
119 of deglaciation (after ~12 kyr) was largely driven by surface melt, which is corroborated by
120 independent modelling of the ice sheet's surface mass balance^{17,22}, and inferences based on
121 the density of subglacial meltwater channels (eskers)²³. Specifically, surface energy balance
122 modelling¹⁷ suggests that a transition from a positive to negative surface mass balance
123 occurred between 11.5 and 9 kyr, when much of the LIS retreat occurred at rates two to five
124 times faster than before 11.5 kyr. In that study¹⁷, volume losses not attributable to surface

125 melting were assumed to be from dynamic discharge and, in broad agreement with our results
126 (Fig. 3f), their modelling implies that dynamic discharge decreased from ~15.5 kyr. Our
127 range of discharge estimates at the LGM (750-2,300 km³) and in the early Holocene (100-700
128 km³ at 9 kyr) also fall within their inferred ranges (770-2,750 km³ and 0-1,650 km³,
129 respectively). The major difference is that their modelling suggests that dynamic discharge
130 increased from the LGM to a maximum (4,290-4,620 km³) around the time of Heinrich event
131 1 (H1: 15.5 kyr) when their modelled surface mass balance is largest. A positive mass
132 balance is temporarily induced in the ice sheet modelling¹⁶ shown in Fig. 3f to facilitate a
133 large dynamic discharge from the Hudson Strait Ice Stream during H1. We do not depict such
134 extreme discharge at this time because our approach is based on modern ice stream data that
135 are unlikely to capture such extreme discharges. However, we find no obvious spatial
136 reorganisation²⁴ of ice streams during or immediately after H1. This suggests that H1 had
137 limited impact on the wider ice sheet drainage network, and points to extreme velocity
138 fluctuations on specific ice streams (e.g. Hudson Strait)²⁵, which we are unable to constrain,
139 and/or mechanisms that do not invoke major ice sheet collapses and jumps in sea level, such
140 as ice shelf break-up²⁶. In contrast, we note some reorganisation of ice streaming following,
141 but not prior to or during, Meltwater Pulse 1A (that began ~14.6 kyr)²⁷. The saddle collapse
142 that occurred during separation of the Laurentide and Cordilleran ice sheets has been
143 hypothesised to have contributed to this event²⁸ and we note several short-lived ice streams in
144 this region after the collapse, but with a concomitant decrease in ice stream activity along the
145 southern margin (Fig. 1c).

146 It is important to consider whether ice streaming in the LIS offers an analogue for
147 modern-day ice sheets. Although the ocean-climate forcing would have been different during
148 deglaciation of the LIS, there is no empirical evidence or theoretical reasoning to suppose
149 that Laurentide ice streams should behave in a fundamentally different manner. Our

150 reconstructed pattern of ice streams at the LGM is remarkably similar to the velocity pattern
151 of the Greenland and Antarctic Ice Sheets, and we note that Laurentide ice streams drained a
152 similar proportion of the ice sheet perimeter, when it was a similar size to present-day
153 Antarctica (Fig. 1a, b). Large sectors of the LIS occupied similar physiography to modern ice
154 sheets, with ice streams exhibiting a similar size, shape and spatial organisation along its
155 marine margins. The most obvious difference is that the LIS retreated onto a low-relief, hard
156 bedrock terrain and had ice streams that terminated on land and produced large, low-relief
157 lobes along much of the southern and western margins^{19,20}. Although these have been likened
158 to some West Antarctic ice streams¹⁹, they have no modern analogue. However, whilst all
159 modern ice streams are marine-terminating, large parts of the Greenland and East Antarctic
160 Ice Sheets will have land-based margins if they continue to deglaciare^{29,30}, which might be
161 within a few millennia in Greenland¹. Our analysis confirms that the geology and topography
162 over which modern-ice sheets retreat will be a key determinant on where ice streams are
163 likely to activate and deactivate⁸. However, we also find a strong dependency between ice
164 sheet volume and ice stream activity that also holds for modern ice sheets (Fig. 4c) and which
165 hints at a more regulatory role in ice sheet dynamics than previously recognised. This does
166 not preclude instabilities at decadal to centennial time-scales⁵⁻⁷, but suggests that if modern
167 ice sheets continue to deglaciare, ice streams are likely to switch off and their relative
168 contribution to mass loss may decrease over several millennia, with final deglaciation
169 accomplished most effectively by surface melt^{17,22}.

170

171 **References:**

- 172 1. Alley, R.B., Clark, P.U., Huybrechts, P. & Joughin, I. Ice-sheet and sea-level changes.
173 *Science* **310**, 456-460 (2005)

- 174 2. Rignot, E. & Kanagaratnam, P. Changes in the velocity structure of the Greenland Ice
175 Sheet. *Science* **311**, 986-990 (2006).
- 176 3. Rignot, H.D. et al. Recent Antarctic ice mass loss from radar interferometry and regional
177 climate modelling. *Nat. Geosci.* **1**, 106-110 (2008).
- 178 4. Rignot, E., Velicogna, I., van den Broeke, M.R., Monaghan, A. & Lenaerts, J.T.M.
179 Acceleration of the contribution of the Greenland and Antarctic ice sheets to sea level
180 rise. *Geophys. Res. Lett.* **38**, L05503 (2011).
- 181 5. Golledge, N.R. et al. The multi-millennial Antarctic commitment to future sea-level rise.
182 *Nature*, **526**, 421-425 (2015).
- 183 6. Feldmann, J. & Levermann, A. Collapse of the West Antarctic Ice Sheet after local
184 destabilization of the Amundsen Basin. *Proc. Nat. Acad. Sci.*, doi:
185 10.1073/pnas.1512482112 (2015).
- 186 7. Joughin, I., Smith, B.E. & Medley, B. Marine ice sheet collapse potentially under way for
187 the Thwaites Glacier Basin, West Antarctica. *Science*, **344**, 735-738 (2014).
- 188 8. Ritz C. et al. Potential sea-level rise from Antarctic ice-sheet instability constrained by
189 observations. *Nature*, doi: 10.1038/nature16147 (2015).
- 190 9. IPCC, 2013: Summary for Policymakers. In, Climate Change 2013: The Physical Science
191 Basis. Contribution of Working Group I to the Fifth Assessment Report of the
192 Intergovernmental Panel on Climate Change [Stocker, T.F., Qin, G.-K. Plattner, M.
193 Tignor, S.K. Allen, J. Boschung, A. Nauels, Y. Xia, V. Bex and P.M. Midgley (eds.)].
194 Cambridge University Press, Cambridge, UK and New York, USA.
- 195 10. Kleman, J. & Applegate, P.J. Durations and propagation patterns of ice sheet instability
196 events. *Quat. Sci. Rev.* **92**, 32-29 (2014)
- 197 11. Rignot, E. Mouginot, J. & Scheuchl, B, Ice flow of the Antarctic ice sheet. *Science*, **333**,
198 1427-1430 (2011).

- 199 12. Rose, K.E. Characteristics of ice flow in Marie Byrd Land. *J. Glaciol.* **24** (90), 63-75
200 (1979).
- 201 13. Nghiem, S.V. et al. The extreme melt across the Greenland ice sheet in 2012. *Geophys.*
202 *Res. Lett.* **39**, L20502 (2012)
- 203 14. Margold, M., Stokes, C.R., Clark, C.D. & Kleman, J. Ice streams in the Laurentide Ice
204 Sheet: a new mapping inventory. *J. Maps* **11** (3), 380-395 (2015).
- 205 15. Dyke, A.S., Moore, A. & Robertson, L. *Deglaciation of North America*. Open File
206 Report, Geological Survey of Canada, Ottawa (2003).
- 207 16. Tarasov, L., Dyke, A.S., Neal, R.M. & Peltier, W.R. A data-calibrated distribution of
208 deglacial chronologies for the North American ice complex from glaciological modelling.
209 *Earth and Plan. Sci. Lett.* **315**, 30-40 (2012).
- 210 17. Ullman, D.J. et al., Laurentide ice-sheet instability during the last deglaciation. *Nat.*
211 *Geosci.*, doi: 10.1038/NGEO2463 (2015).
- 212 18. Winsborrow, M.C.M., Clark, C.D. & Stokes, C.R. What controls the location of ice
213 streams? *Earth-Sci. Rev.* **103**, 45-59 (2010).
- 214 19. Clark, P.U. Surface form of the southern Laurentide Ice Sheet and its implications to ice-
215 sheet dynamics. *Geol. Soc. Am. Bull.* **104**, 595-605 (1992).
- 216 20. Ó Cofaigh, C., Evans, D.J.A. and Smith, I.R. Large-scale reorganisation and
217 sedimentation of terrestrial ice streams during late Wisconsinan Laurentide Ice Sheet
218 deglaciation. *Geol. Soc. Am. Bull.* **122** (5-6), 743-756 (2010).
- 219 21. Stokes, C.R. & Clark, C.D. Laurentide ice streaming over the Canadian Shield: a conflict
220 with the soft-bedded ice stream paradigm? *Geology* **31** (4), 347-350 (2003).
- 221 22. Carlson, A.E. et al. Surface-melt driven Laurentide Ice Sheet retreat during the early
222 Holocene. *Geophys. Res. Lett.* **26** (24), L24502 (2009).

- 223 23. Storrar, R.D., Stokes, C.R. & Evans, D.J.A. Increased channelization of subglacial
224 drainage during deglaciation of the Laurentide Ice Sheet. *Geology*, **42** (3), 239-242
225 (2014).
- 226 24. Mooers, H.D. & Lehr, J.D. Terrestrial record of Laurentide Ice Sheet reorganisation
227 during Heinrich events. *Geology* **25** (11), 987 (1997).
- 228 25. Hemming, S.R. Heinrich events: massive late Pleistocene detritus layers of the North
229 Atlantic and their global climate imprint. *Revs. Geophys.*, **42**, RG1005 (2004).
- 230 26. Marcott, S.A. et al. Ice-shelf collapse from subsurface warming as a trigger for Heinrich
231 events. *Proc. Nat. Acad. Sci.* 108 (33), 13415-13419 (2011).
- 232 27. Deschamps, P. et al. Ice-sheet collapse and sea-level rise at the Bolling warming 14,600
233 years ago. *Nature* **483** (7391), 559-564 (2012).
- 234 28. Gregoire, L., Payne, A.J. & Valdes, P.J. Deglacial rapid sea level rises caused by ice-
235 sheet saddle collapses. *Nature* **487**, 219-222 (2012).
- 236 29. Bamber, J.L. et al. A new bed elevation dataset for Greenland. *The Cryosphere* **7**, 499-
237 510 (2013).
- 238 30. Fretwell, P. et al. Bedmap 2: improved ice bed, surface and thickness datasets for
239 Antarctica. *The Cryosphere* **7**, 373-393 (2013).

240

241 **Supplementary Information** is available.

242

243 **Acknowledgements:**

244 This research was funded by a Natural Environment Research Council award NE/J00782X/1
245 (C.R.S & C.D.C.). Landsat imagery and the GTOPO30 digital elevation model were provided
246 free of charge by the US Geological Survey Earth Resources Observation Science Centre.

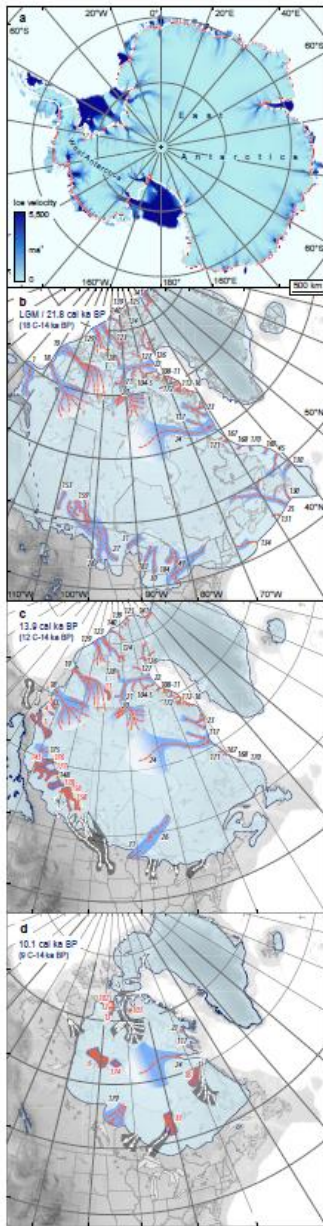
247

248 **Author contributions:**

249 C.R.S. conceived the study and wrote the proposal with C.D.C. M.M. generated the data on
250 the timing of palaeo-ice streams, modern-ice stream discharge, palaeo-ice stream discharge,
251 and produced the Figures and Supplementary Information, with input from C.R.S. and C.D.C.
252 L.T contributed data from numerical modelling. All authors contributed to the analyses and
253 interpretations of the data. C.R.S. wrote the manuscript with input from all authors.

254

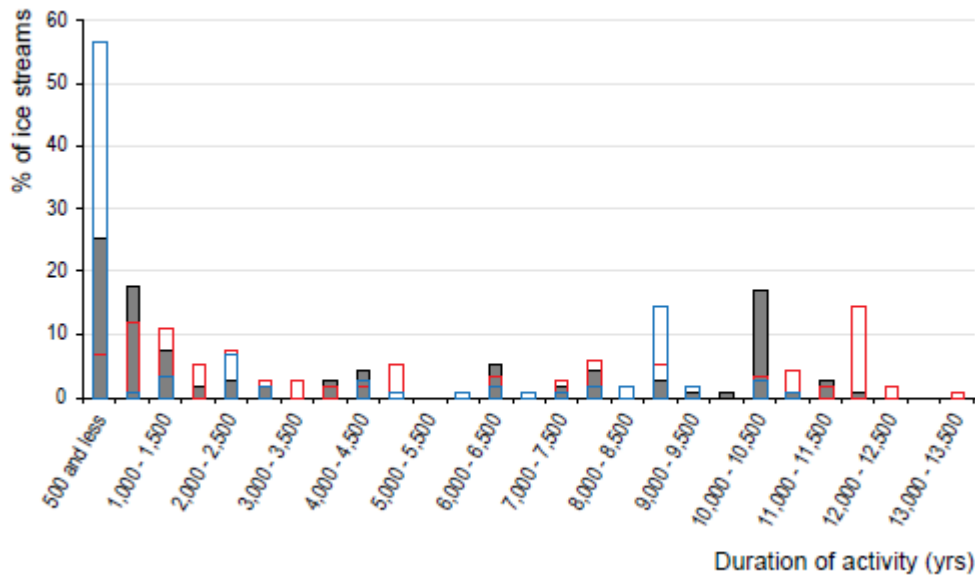
255 **Author information:** Reprints and permissions information is available at
256 www.nature.com/reprints. The authors declare no competing financial interests. Readers are
257 welcome to comment on the online version of the paper. Correspondence and requests for
258 materials should be addressed to C.R.S. (c.r.stokes@durham.ac.uk).



260

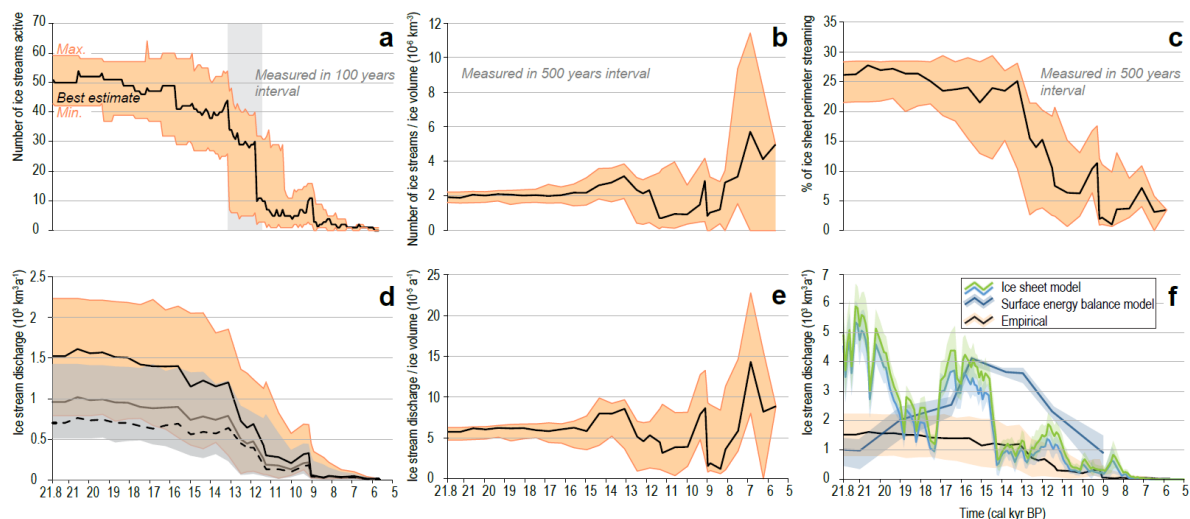
261 **Figure 1: Ice flow velocity of the Antarctic ice sheet¹¹ compared (at the same scale) with**
 262 **reconstructions of ice stream activity in the LIS at selected time-steps. (a)** Present-day
 263 Antarctic ice sheet velocity¹¹ with red lines indicating where ice streams intersect the
 264 grounding line. Ice streams reconstructed for the LIS at (b) the LGM (~21.8 kyr), (c) 13.9
 265 kyr, and (d) 10.1 kyr. Laurentide ice stream locations in light blue (numbers from the
 266 inventory¹⁴), with those that switched off within the preceding 1,000 years in grey, and those
 267 that switched on during the following 1,000 years in dark blue. Underlying topography (b, c
 268 and d) from GTOPO30 digital elevation data.

269



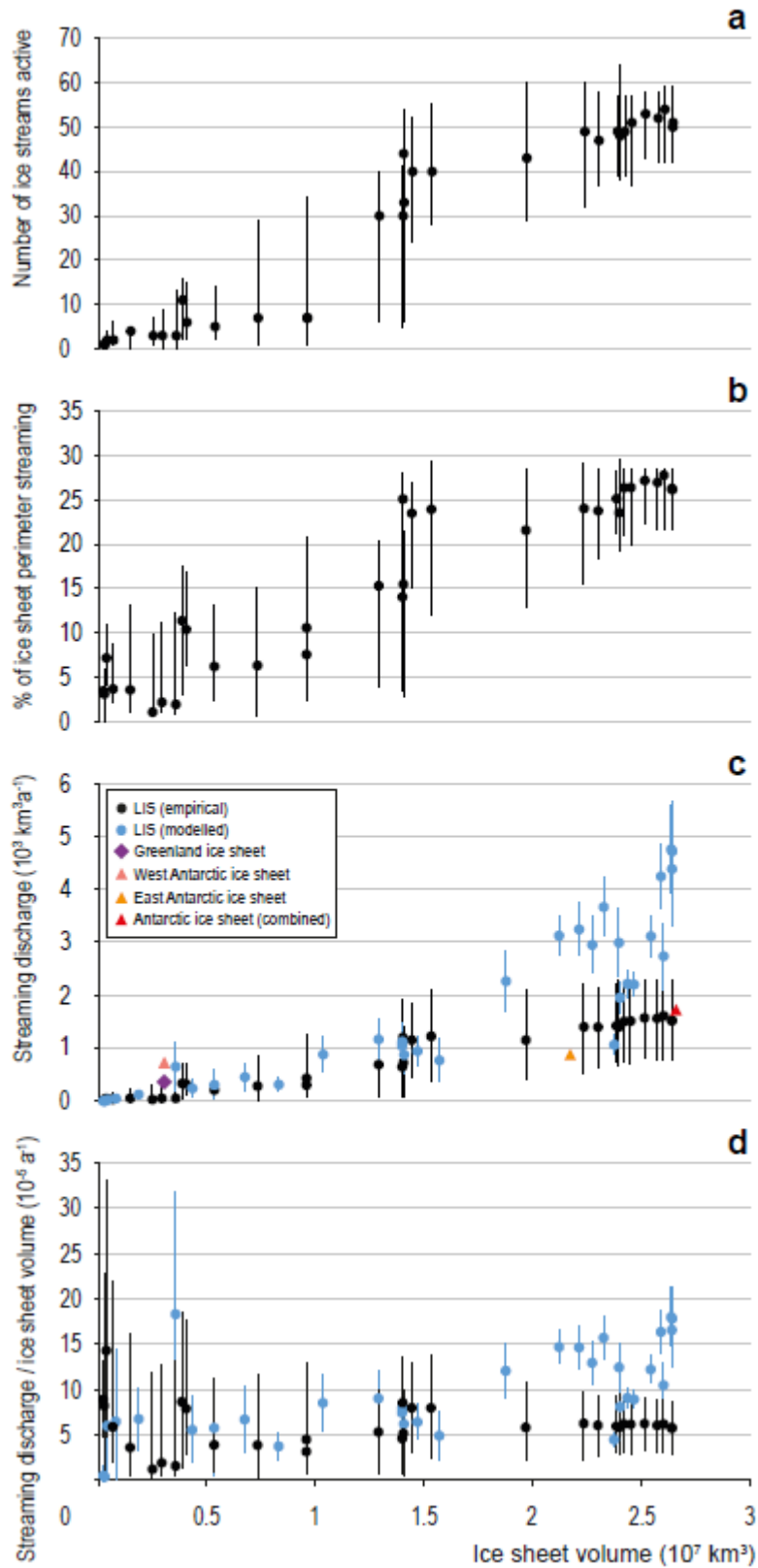
270

271 **Figure 2: Duration of individual ice streams in the LIS.** Grey-filled bars are the data for
 272 the best estimate of each ice stream’s duration, with blue outlines representing data if the
 273 minimum duration is assumed for all ice streams, and red outlines if the maximum duration is
 274 assumed for all ice streams (see [Extended Data Figure 1](#) for ice stream locations).
 275



276

277 **Figure 3: Ice stream activity during deglaciation of the Laurentide Ice Sheet (LIS).** (a)
 278 Number of ice streams active during deglaciation, with orange shading indicating the
 279 uncertainty in the age-bracketing of ice streams and grey vertical bar showing the time when
 280 the ice sheet margin transitioned from a predominantly soft to predominantly hard bed. (b)
 281 Number of active ice streams normalised by LIS volume obtained from a data-calibrated
 282 numerical modelling¹⁶. Orange shading indicates uncertainty in the age-bracketing of ice
 283 streams. (c) Percentage of the ice sheet perimeter that was streaming, with orange shading
 284 indicating uncertainty in the age-bracketing of ice streams. (d) First-order estimate of the
 285 total ice stream discharge based on a width-discharge regression from modern-ice stream data
 286 (see Methods). Orange shading indicates the uncertainty in both the age-bracketing of the ice
 287 streams and the discharge uncertainty from the 95% confidence intervals of the regression.
 288 For comparison, grey shading shows the range of discharges obtained using the regression
 289 without two obvious outliers (Extended Data Figure 10). Dashed line shows discharge from
 290 a cruder two state approximation for the best estimate of ice stream duration (see Methods).
 291 (e) Ice stream discharge (black line in d) normalised by LIS volume from numerical
 292 modelling¹⁶. Orange shading indicates the uncertainty in the age-bracketing of ice streams.
 293 (f) Empirical ice discharge (from d) compared to ice stream discharge generated from the
 294 mean of a data-calibrated numerical modelling ensemble of the LIS¹⁶. Light blue line shows
 295 streaming discharge from grounded ice-margin grid cells with velocities $>500 \text{ m a}^{-1}$ and
 296 green for grounded margin grid cells $>100 \text{ m a}^{-1}$ (both with 1-sigma uncertainties). Dark blue
 297 shows discharge inferred from previous modelling of the ice sheet's surface mass balance¹⁷.
 298



299
300

301 **Figure 4: Indicators of ice stream activity plotted against ice sheet volume.** (a) Number
 302 of ice streams plotted against ice sheet volume. Black dots show results using best estimates
 303 of ice stream duration with vertical lines showing the uncertainty in the age-bracketing. (b)

304 Percentage of the ice sheet perimeter that was streaming plotted against ice sheet volume
305 (symbols as in (a)). (c) Total ice stream discharge plotted against ice sheet volume using our
306 empirical calculations (black dots show best estimate and lines show both the age and
307 discharge uncertainties from Fig. 3d) and total ice stream discharge from numerical
308 modelling¹⁶ (blue dots show mean and lines show 2-sigma uncertainties). Modelled discharge
309 is extracted from grounded ice-marginal grid-cells with velocities $>500 \text{ m a}^{-1}$ (blue line in
310 Fig. 3f). Data for the present-day ice sheets in Greenland (purple diamond), West Antarctica
311 (pink triangle), East Antarctica (orange triangle) and West and East Antarctica combined (red
312 triangle) are also plotted using recent ice stream discharge^{2,3} and ice sheet volume^{29,30}
313 estimates. (d) Total ice stream discharge from modelled and empirical estimates in (c)
314 normalised by ice sheet volume and plotted against ice sheet volume. In all panels, ice sheet
315 volume is derived from the mean of a best-performing ensemble of previously-published
316 data-calibrated numerical modelling¹⁵ (see Methods). Note that the low modelled streaming
317 fraction at volumes around $2.4 \times 10^7 \text{ km}^3$ (c & d) are due to the dynamic facilitation of
318 Heinrich event 1 in that modelling (see Methods). Empirical discharges for small ice volumes
319 ($< 0.2 \times 10^7 \text{ km}^3$) have highly under-represented uncertainties given higher ice sheet volume
320 uncertainties close to final deglaciation.

321

322

323 **METHODS:**

324 **Identifying palaeo-ice stream locations:** An ice stream is a region in a grounded ice sheet
325 that flows much faster than the regions on either side³¹. Where the fast-flowing ice becomes
326 bordered by exposed rock (e.g. in high relief fjord landscapes) they are usually referred to as
327 marine-terminating outlet glaciers. These outlet glaciers typically initiate as ice streams and
328 so we use the term ‘ice stream’ throughout, but include outlet glaciers.

329 We use a recently-published inventory¹⁴ of palaeo-ice streams in the Laurentide Ice
330 Sheet (LIS), which includes 117 ice streams ([Extended Data Figure 1](#)). These were identified
331 based on previously published evidence, complemented with new mapping using satellite
332 imagery and Digital Elevation Models (DEMs) on land, and bathymetric data and swath
333 bathymetry for submerged areas¹⁴. The systematic nature of the new mapping from across the
334 entire ice sheet bed means it is very unlikely that any major ice streams have been missed¹⁴.

335 Ice streams are easily distinguishable on a palaeo-ice sheet bed from a variety of
336 evidence that is now well-established in the literature^{14,20,21,32-43}. Their spatially discrete
337 enhanced flow creates a distinctive bedform imprint that is immediately recognisable and
338 characterised by several geomorphological criteria³². These include highly elongated
339 subglacial bedforms (mega-scale glacial lineations³⁴: [Extended Data Figures 4 & 5](#)), which
340 have also been observed beneath modern ice streams³⁵, and these bedforms typically exhibit
341 convergent flow patterns towards a main ice stream ‘trunk’. These landform assemblages are
342 often characterised by abrupt lateral margins that border areas with much shorter subglacial
343 bedforms, or no bedforms at all^{32,33,36,37,42,43} ([Extended Data Figure 5](#)). In some cases, the
344 abrupt margin is marked by features known as ice stream shear margin moraines^{32,33,37,38}
345 ([Extended Data Figure 5](#)). This landform evidence is readily identifiable on satellite imagery
346 and aerial photographs^{32,34,36-39,43} and, in some cases, is further augmented by field
347 investigations that reveal discrete (Boothia-type)³³ erratic dispersal trains or sedimentological
348 evidence from tills that may have been overridden and/or deformed by rapid ice flow.
349 However, there are no ice streams in the inventory that are based only on sedimentological
350 data and most (>85%) have a clear bedform imprint¹⁴.

351 At a larger spatial scale, it is known that many ice streams are steered by the
352 underlying topography, often forming marine-terminating outlet glaciers bordered by rock
353 walls²⁻⁴. The inventory includes these topographic ice streams, many of which were identified
354 by major cross shelf-troughs and their associated sedimentary depocentres⁴⁰ ([Extended Data](#)
355 [Figure 6](#)). Swath bathymetry from within these troughs commonly reveals many of the
356 geomorphological criteria³² described above, such as mega-scale glacial lineations^{34,35,42}.

357 Given previous work that highlights the importance of ‘soft’ bedrock geology in
358 influencing ice stream location^{10,18,19}, we also analysed the type of bedrock over which each
359 ice stream was located. We categorized their underlying geology as either (i) predominantly
360 ‘soft’ sedimentary rocks, (ii) predominantly ‘hard’ crystalline rocks (intrusive, metamorphic
361 and volcanic rocks) or (iii) those where the spatial footprint of the ice stream extended over a
362 mixture of both soft and hard rocks. This allowed us to calculate the number of different
363 types of ice streams on each broad geological category through time ([Extended Data Figure](#)
364 [3](#)).

366 **Dating palaeo-ice streams:** We used the best-available pan-ice sheet margin chronology¹⁵ to
367 bracket the age of the spatial footprints of each ice stream in the inventory¹⁴. The ice margin
368 chronology includes 32 time-steps, starting at 21.8 kyr (18 14C yr), ending at 5.7 kyr (5 14C
369 yr), and based on >4,000 dates that are spread across the entire ice sheet bed ([Extended Data
370 Figure 2](#)). The database consists of mainly radiocarbon dates, supplemented with varve and
371 tephra dates, which constrain ice margin positions, and shorelines of large glacial lakes. Dates
372 on problematic materials (e.g. marl, freshwater shells, lake sediment with low organic carbon
373 content, marine sediment, bulk samples with probable blended ages, and most deposit feeding
374 molluscs from calcareous substrates) were excluded. Marine shell dates, a major component,
375 were adjusted for regionally variable marine reservoir effects based on a large new set of
376 radiocarbon ages on live-collected, pre-bomb molluscs from Pacific, Arctic, and Atlantic
377 shores. We use a mixed marine and Northern Hemisphere atmosphere calibration curve while
378 Dyke et al.¹⁵ used IntCal98 calibration curve.

379 We used the ice margin chronology to bracket the duration of ice stream activity using
380 methods employed in previous work on individual or small numbers of ice streams^{21,36,41-43}
381 ([Extended Data Figure 7](#)). In some cases, the duration of ice streaming may have been short-
382 lived (just few hundred years), leaving evidence of a simple ‘rubber-stamped’ imprint³² of
383 their activity, the spatial extent of which can be readily matched to just one or two ice margin
384 positions ([Extended Data Figure 7a](#)). The more complex landform assemblages of other ice
385 streams (with overprinted MSGLs linked to associated ice marginal features) clearly indicate
386 that they continued to operate during ice margin retreat ([Extended Data Figure 7b](#)), and we
387 therefore fit the ice stream activity to a series of ice margin positions over a longer-timespan
388 (hundreds to thousands of years). Similar patterns are seen for marine-terminating ice
389 streams⁴² ([Extended Data Figure 7c and 7d](#)).

390 To account for the inherent uncertainties in the dating (and interpolated ice margin
391 position) and the spatial extent of each ice stream, we provide a maximum possible duration
392 and a minimum duration for each ice stream in the inventory ([Figure 2](#)). It should be noted
393 that in some cases where the interpolated ice margin positions indicated a very short duration
394 of ice streaming, we set the minimum duration to 100 years. This is because the creation of
395 subglacial bedforms that permits their identification is likely to be of the order of decades³⁵
396 and attempting to date to a higher precision is meaningless given the dating uncertainties
397 (mainly radiocarbon) and our focus on millennial-scale changes throughout deglaciation.

398
399 **Estimating palaeo-ice stream discharges:** Unfortunately, there is no direct means to
400 empirically reconstruct the velocity, and thus discharge, of a palaeo-ice stream from the
401 evidence it left behind. In order to provide a simple, first-order estimate of the potential ice
402 discharge from each palaeo-ice stream where only the width is known confidently, we used
403 an empirical relationship between the width and discharge of 81 active ice streams in
404 Antarctica (50: [Extended Data Figure 8](#)) and Greenland (31: [Extended Data Figure 9](#)). Ice
405 velocities (m a⁻¹) were extracted from recent compilations in Greenland (2008-2009)⁴⁴ and
406 Antarctica (2007-2009)⁴⁵ and we used these velocity datasets to measure the width (km) of

407 the ice stream (to the lateral shear margins or exposed rock walls) at the grounding line^{29,45}.
408 Velocity was extracted as a width-averaged value. We then used the highest resolution bed-
409 data that was available for Greenland²⁹ and Antarctica³⁰ to calculate the cross-sectional area
410 (km²) of each ice stream at the grounding line. We then calculated the modern ice stream
411 discharge (km³ a⁻¹) by multiplying the velocity data by the ice-thickness data and integrating
412 the output along the ice stream's width at the grounding line.

413 When ice stream data from Antarctica and Greenland are amalgamated ([Extended](#)
414 [Data Figure 10](#)), a simple linear regression reveals a weak correlation ($R^2 = 0.39$) between
415 their width and discharge, which we use to predict an order-of-magnitude palaeo-discharge
416 from the width of each palaeo-ice stream that was active during deglaciation at each dated
417 margin position ([Figure 3d](#)). The regression is clearly influenced by two outliers with
418 extremely high discharge (Pine Island Glacier and Thwaites Glacier, West Antarctica).
419 Without them, the correlation weakens ($R^2 = 0.31$) and our palaeo-discharge estimates show
420 the same trend, but absolute discharges are lower (see grey shading on [Fig. 3d](#)). We
421 considered removing them from the regression, but use them in our estimates of palaeo-
422 discharge (e.g. in [Fig. 3e](#) and [f](#), and [Fig. 4c](#) and [d](#)) because they allow us to partly capture
423 some of the more extreme discharges that might be expected in a deglaciating ice sheet. We
424 also extract the 95% confidence intervals of the regression and use these to estimate a lower
425 and upper range of discharge for an ice stream of given width. It should be noted, however,
426 that these confidence intervals under-represent the uncertainty because some assumptions for
427 those confidence intervals (and the general validity of linear regression) are broken: a)
428 Gaussian noise, b) no correlation between individual data point residuals, c) constant
429 variance. Given this, and the obvious (and perhaps not surprising) complexity of the
430 relationship between discharge and width for modern ice streams (e.g. the mean value of
431 linear ice stream flux for Greenlandic ice streams is very different from that for Antarctic ice
432 streams, where there is a stronger relationship), we also extract a discharge relationship with
433 a cruder two state approximation that avoids the assumptions required for statistically robust
434 application of linear regression. It is also important to note that the modern ice stream data
435 are from one short time-period and yet we know that ice streams with a fixed width can
436 accelerate (and decelerate) at short (annual-decadal) time-scales²⁻⁴. However, the extent to
437 which these accelerations and decelerations are sustained over longer (centennial-millennial)
438 time-scales is presently unknown. Thus, we use this simple approach to generate the first
439 empirical order-of-magnitude estimate of palaeo-discharge from the LIS averaged over
440 millennial time-scales and note that our empirical results are broadly similar to those
441 generated by numerical modelling^{16,17} ([Fig. 3f](#)), albeit typically lower.

442 To evaluate our empirical estimates of palaeo-ice stream discharge in relation to ice
443 sheet volume (e.g. [Fig's 3d, 3e](#) and [Fig. 4](#)), we extracted ice sheet volume from the mean of
444 an ensemble of best-performing model runs from a previously-published data-calibrated
445 numerical model¹⁶. Uncertainties associated with the modelled ice volumes (see Ref. 15) are
446 an order of magnitude less than those associated with our estimates of palaeo-ice stream
447 discharge and are not shown (e.g. in [Fig. 4](#)). We use this same model to compare our
448 empirical estimates of ice stream discharge against those generated in a numerical model of

449 the LIS, with streaming discharge extracted from an ensemble of best-performing model runs
450 at 100 year time-steps during deglaciation from 21.8 to 5.7 kyr, and ensemble standard
451 deviation in ice stream discharge shown in shading around the mean (Fig. 3f). The weighted
452 ensemble mean from this model shows a similar trend of decreasing discharge from ice
453 streams (Fig. 3f), but with higher discharges and greater variability. This is to be expected
454 because our estimates based on modern ice stream discharges may not capture the full range
455 of ice stream behaviour during deglaciation of a mid-latitude ice sheet (e.g., we have no
456 modern analogue of an extensive land-terminating margin overlying soft sediments). It
457 should also be noted that the numerical modelling imposes a data-calibrated reduction in ice
458 streaming around the Hudson Strait region just prior to Heinrich event 1 in order to facilitate
459 a dynamic destabilisation during H1. This is reflected in the reduced streaming discharge in
460 that model for a few thousand years prior to 17 ka and a temporary increase thereafter (Fig. 3f
461 and Fig. 4c and d). It is also reflected in the low modelled streaming fraction at volumes
462 around $2.4 \times 10^7 \text{ km}^3$ (see Fig. 4d).

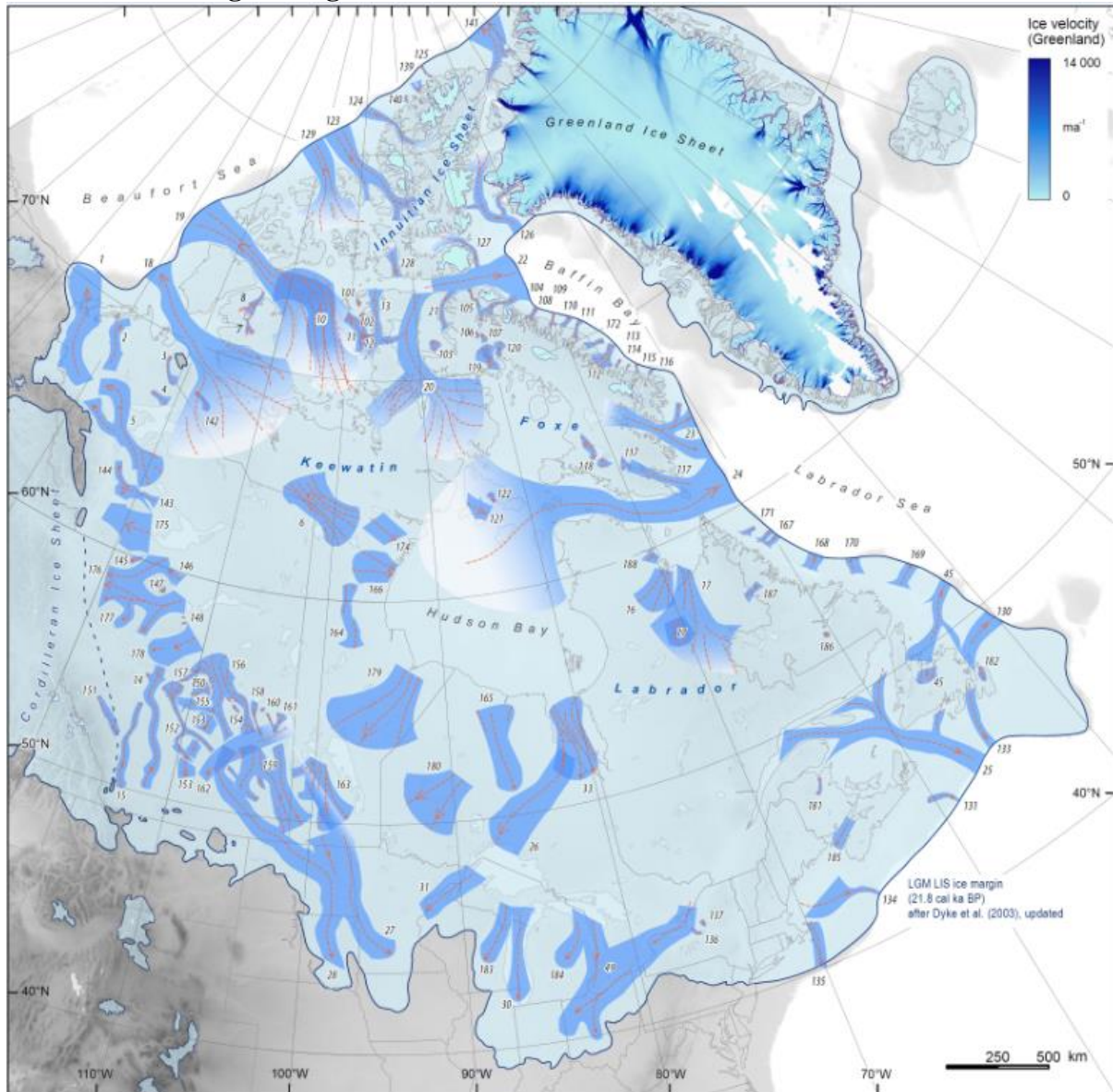
463

464 **Methods References**

- 465 31. Patterson, W.S.B. *The Physics of Glaciers* (3rd Ed). Pergamon, UK (1994).
- 466 32. Stokes, C.R. & Clark, C.D. Geomorphological criteria for identifying Pleistocene ice
467 streams. *A. Glac.* **28**, 67-75 (1999).
- 468 33. Dyke, A.S. & Morris, T.F. Canadian landform examples. 7. Drumlin fields, dispersal
469 trains, and ice streams in Arctic Canada. *Can. Geogr.* **32** (1), 86-90 (1988).
- 470 34. Clark, C.D. Mega-scale glacial lineations and cross-cutting ice flow landforms. *Earth*
471 *Surf. Proc. Land.* **18** (1), 1-29 (1993).
- 472 35. King, E.C. Hindmarsh, R.C.A. & Stokes, C.R. Formation of mega-scale glacial lineations
473 observed beneath a West Antarctic ice stream. *Nat. Geosci.* **2** (8), 585-588 (2009).
- 474 36. Clark, C.D. & Stokes, C.R. Extent and basal characteristics of the M'Clintock Channel
475 Ice Stream. *Quat. Int.* **86** (1), 81-101 (2001).
- 476 37. Hodgson, D.A. Episodic ice streams and ice shelves during retreat of the
477 northwesternmost sector of the late Wisconsinan Laurentide Ice Sheet over the central
478 Canadian Arctic Archipelago. *Boreas* **23** (1), 14-28 (1994).
- 479 38. Stokes, C.R. & Clark, C.D. Ice stream shear margin moraines. *Earth Surf. Proc. Land.* **27**
480 (5), 547-558 (2002)
- 481 39. Stokes, C.R. Identification and mapping of palaeo-ice stream geomorphology from
482 satellite imagery: implications for ice stream functioning and ice sheet dynamics. *Int. J.*
483 *Remote Sens.* **23** (8), 1557-1563 (2002).
- 484 40. Batchelor, C.L. & Dowdeswell, J.A. The physiography of high Arctic cross-shelf troughs.
485 *Quat. Sci. Rev.* **92**, 68-96 (2014).
- 486 41. Stokes, C.R. & Clark, C.D. Palaeo-ice streams. *Quat. Sci. Rev.* **20** (13), 1437-1457
487 (2001).
- 488 42. O'Cofaigh, C., Dowdeswell, J.A., Evans, J. & Larter, R.D. Geological constraints on
489 Antarctic palaeo-ice stream retreat. *Earth. Surf. Proc. Land.* **33** (4), 513-525 (2008).

- 490 43. Stokes, C.R., Clark, C.D. & Storrar, R.D. Major changes in ice stream dynamics during
491 deglaciation of the north-western margin of the Laurentide Ice Sheet. *Quat. Sci. Rev.* **28**
492 (7), 721-738 (2009).
- 493 44. Joughin, I., Smith, B., Howat, I. & Scambos, T. MEaSURES Greenland Ice Sheet
494 Velocity Map from InSAR Data. National Snow and Ice Data Center, Boulder, Colorado
495 USA (2010).
- 496 45. Rignot, E., Mouginot, J. & Scheuchl, B. MEaSURES InSAR-Based Antarctica Ice
497 Velocity Map. National Snow and Ice Data Center, Boulder, Colorado USA (2011).
- 498 46. Rignot, E., Mouginot, J. & Scheuchl, B. Antarctic grounding line mapping from
499 differential satellite radar interferometry. *Geophys. Res. Lett.*, **38** (10): L10504 (2011).
- 500

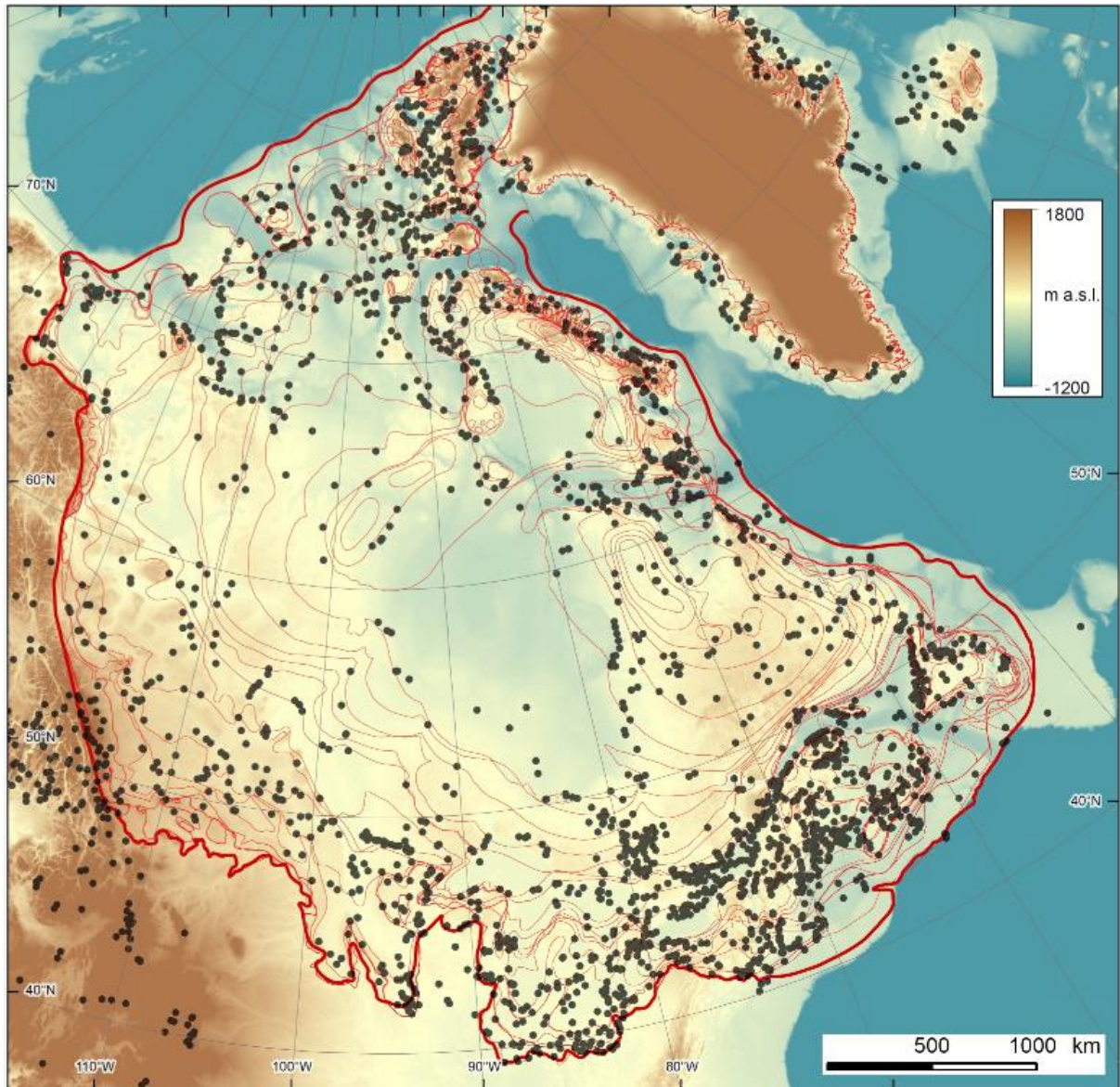
501 **Extended Data Figure Legends:**



502

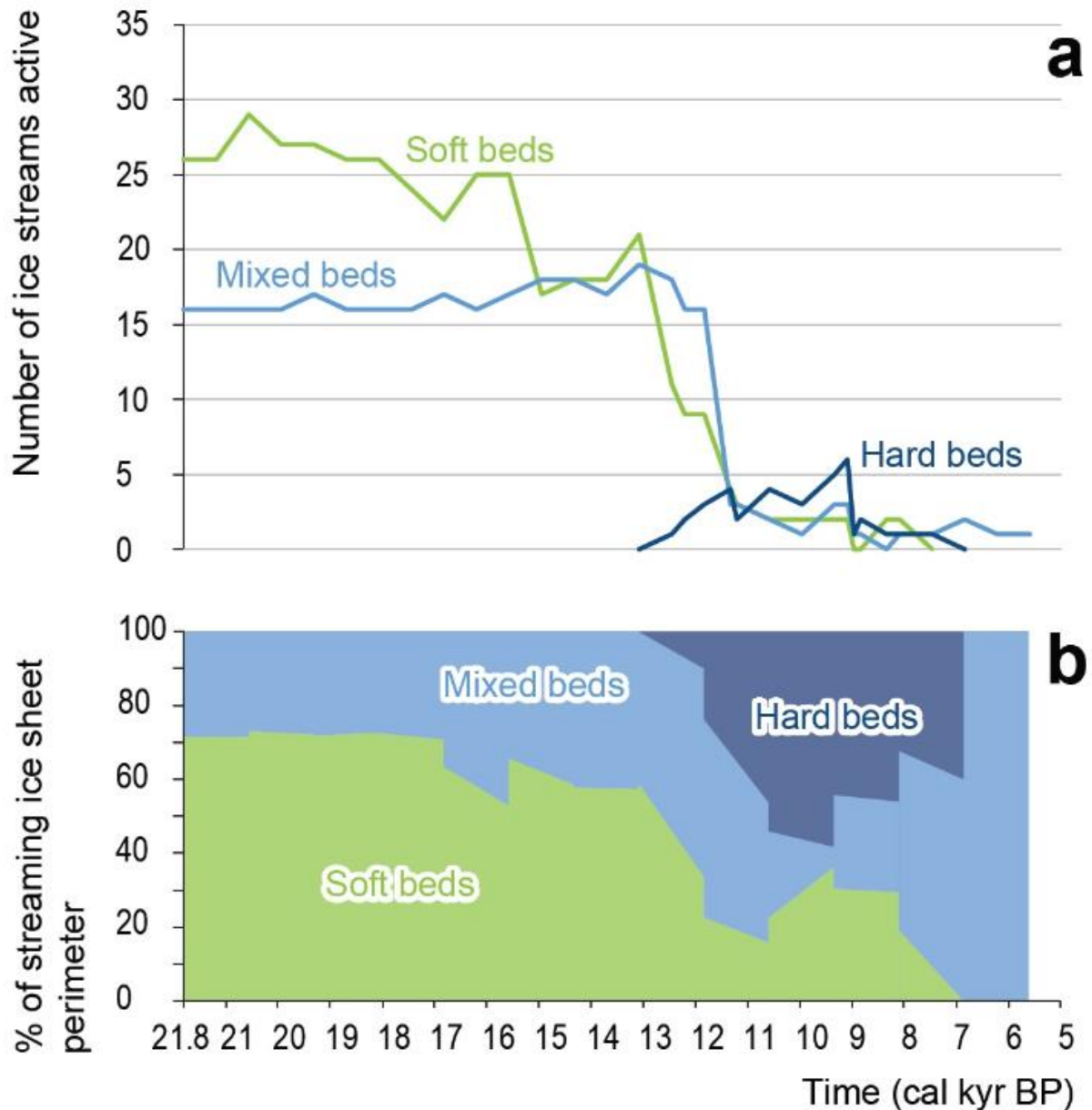
503 **Extended Data Figure 1: Location of 117 ice streams from a recently-compiled**
504 **inventory¹⁴ based on previous work and systematic mapping across the ice sheet bed.**
505 Palaeo-ice streams are shown in dark blue shading and numbered as in ref. 14. Modern-day
506 ice velocity is shown for Greenland⁴⁴. Underlying topography from GTOPO30 digital
507 elevation data⁴⁷.

508



509
510

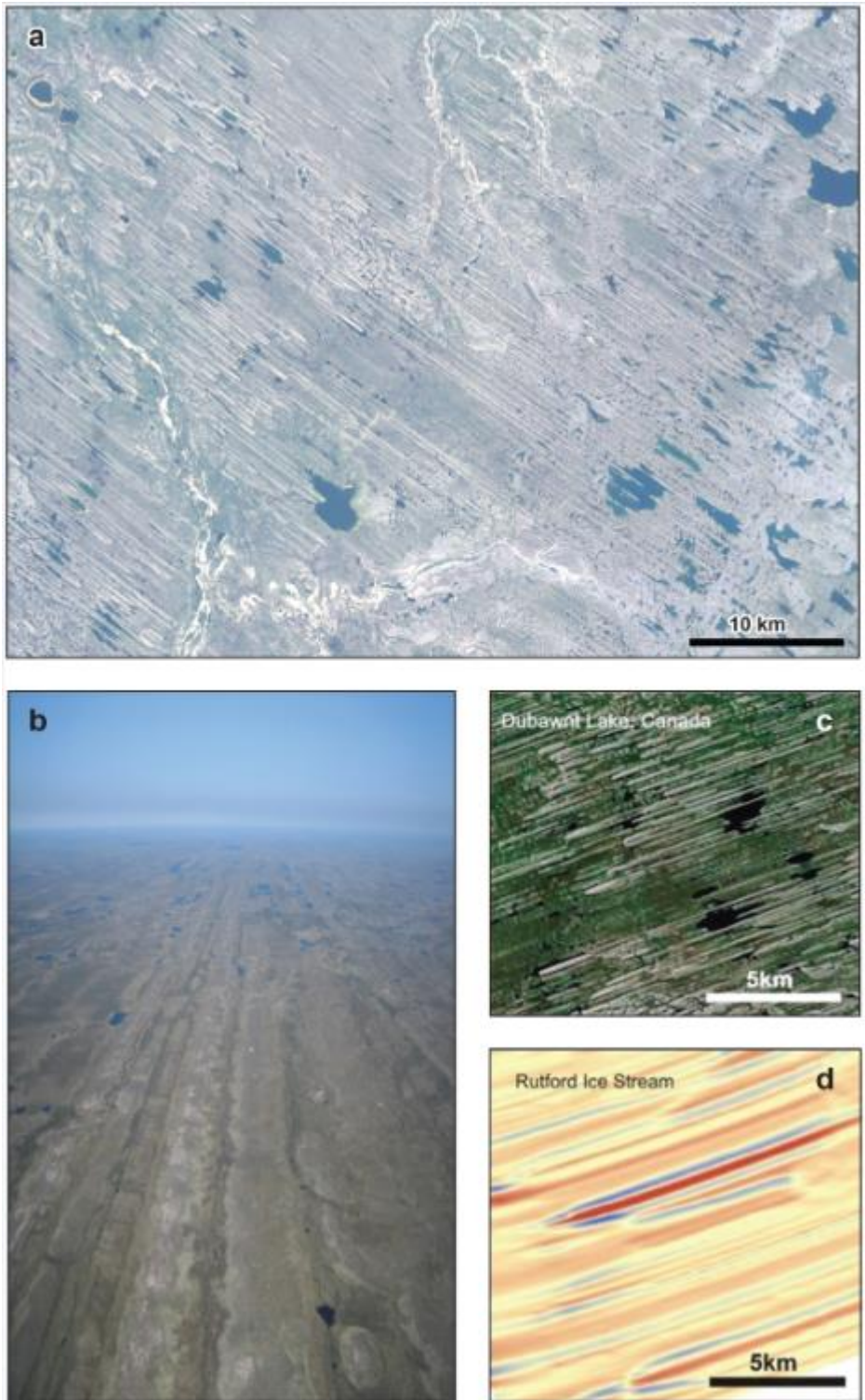
511 **Extended Data Figure 2: Distribution of dates and interpolated ice margin positions**
 512 **from Dyke et al. (2003)¹⁴.** These ice margin positions (thin red lines) are based on dates
 513 (black dots) that we used to bracket the age of the spatial footprint of each ice stream
 514 ([Extended Data Figure 7](#)). The thick red line shows the updated LGM ice margin (following
 515 recent work⁴⁹⁻⁵⁵). Underlying topography from GTOPO30 digital elevation data⁴⁷.
 516



517

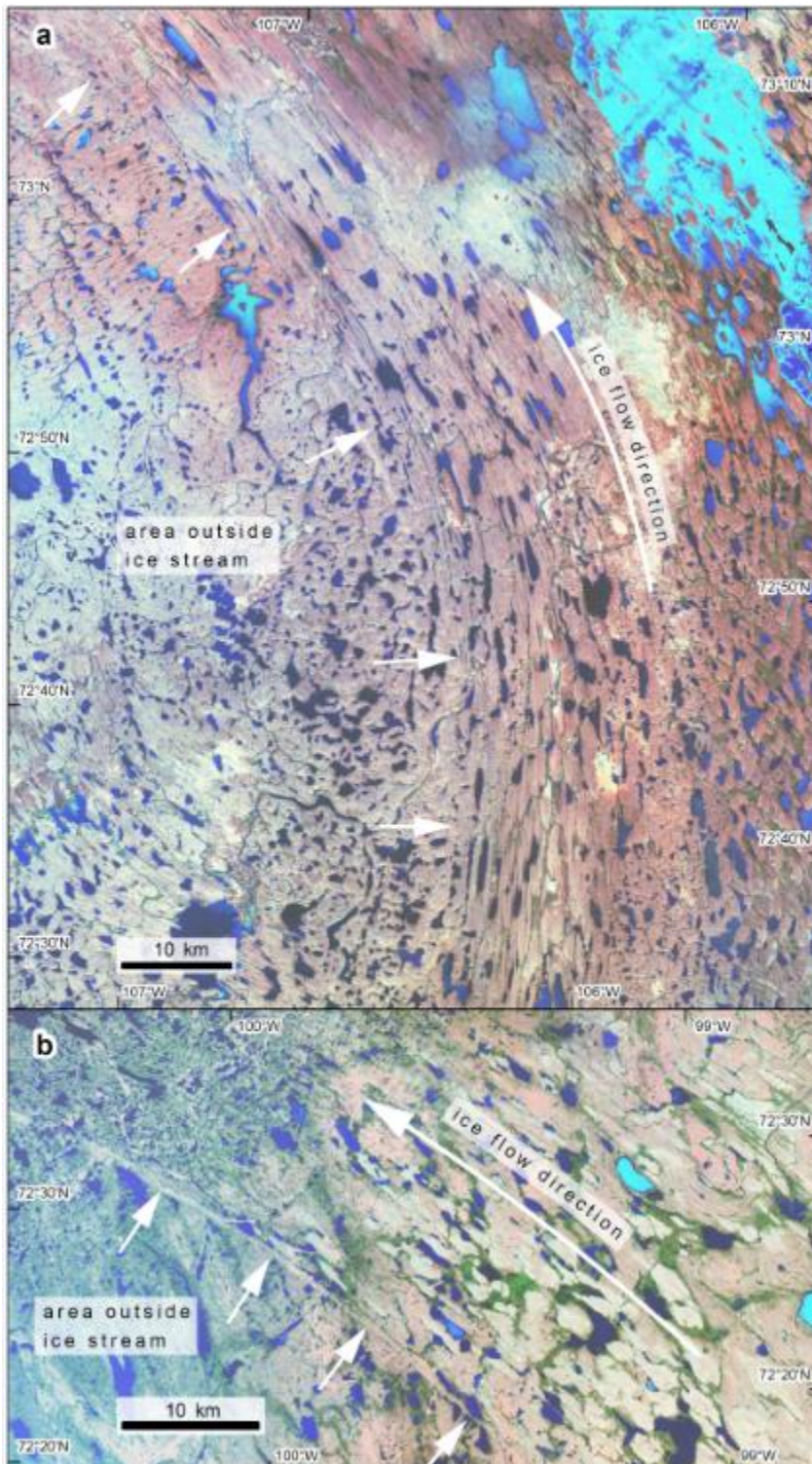
518 **Extended Data Figure 3: The number of ice streams and the percentage of the margin**
 519 **they drained through time, classified according to their underlying geology. (a)** A sharp
 520 drop in the number of ice streams is observed after ~12 kyr (Fig. 3a) which is linked with the
 521 retreat onto the hard crystalline rocks of the Canadian Shield¹⁹. **(b)** Note, however, that
 522 several large, wide ice streams were active over the hard bed geology (e.g. refs. 10, 21) and
 523 they drained a large percentage of the ice sheet's perimeter.

524



525

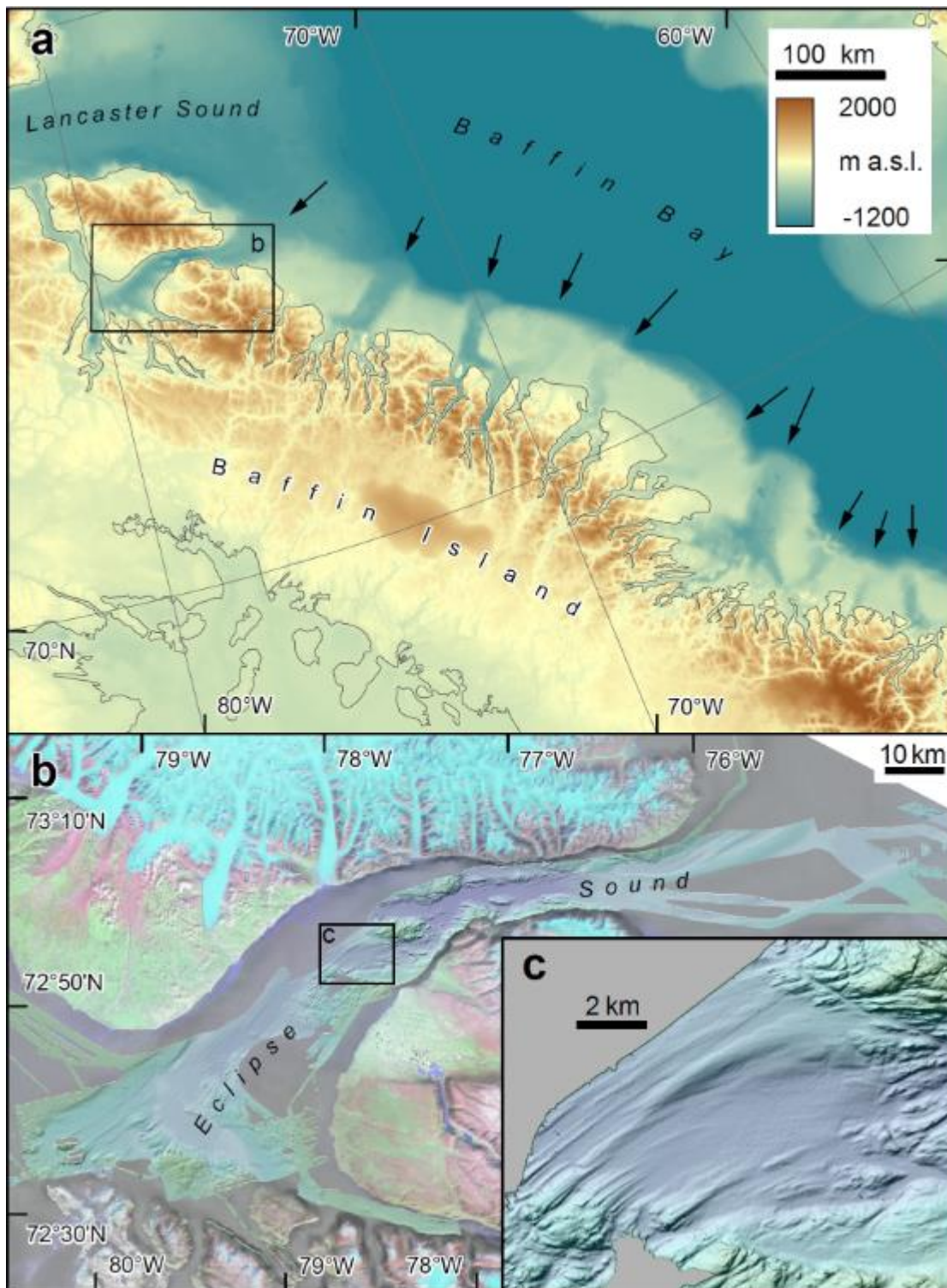
526 **Extended Data Figure 4: Mega-scale glacial lineations³⁴ on the Dubawnt Lake Ice**
 527 **Stream bed²¹, central Canada.** These features are a characteristic geomorphological
 528 signature of ice streaming and are readily identifiable on Landsat satellite imagery (**a** and **c**)
 529 and oblique aerial photography (**b**) of the ice stream bed (no. 6 on [Extended Data Figure 1](#)).
 530 Identical features have been detected beneath Rutford Ice Stream in West Antarctica³⁵ in (d).
 531 Landsat imagery courtesy of the US Geological Survey Earth Resources Observation Science
 532 Centre and photograph by Chris Stokes. Images in (c) and (d) modified from ref. 35.



534

535 **Extended Data Figure 5: Landsat imagery of lateral shear margin moraines in the**
 536 **Canadian Arctic Archipelago. (a) The M'Clintock Channel Ice Stream bed^{36,37} on Victoria**
 537 **Island (no. 10 on [Extended Data Fig. 1](#)), and (b) the Crooked Lake Ice Stream³³ on Prince of**
 538 **Wales Island (no 11 on [Extended Data Fig. 1](#)). Note the abrupt lateral margins (marked by**
 539 **white arrows) of the assemblage of mega-scale glacial lineations that is, in places, marked by**
 540 **lateral shear margin moraines³⁸.**

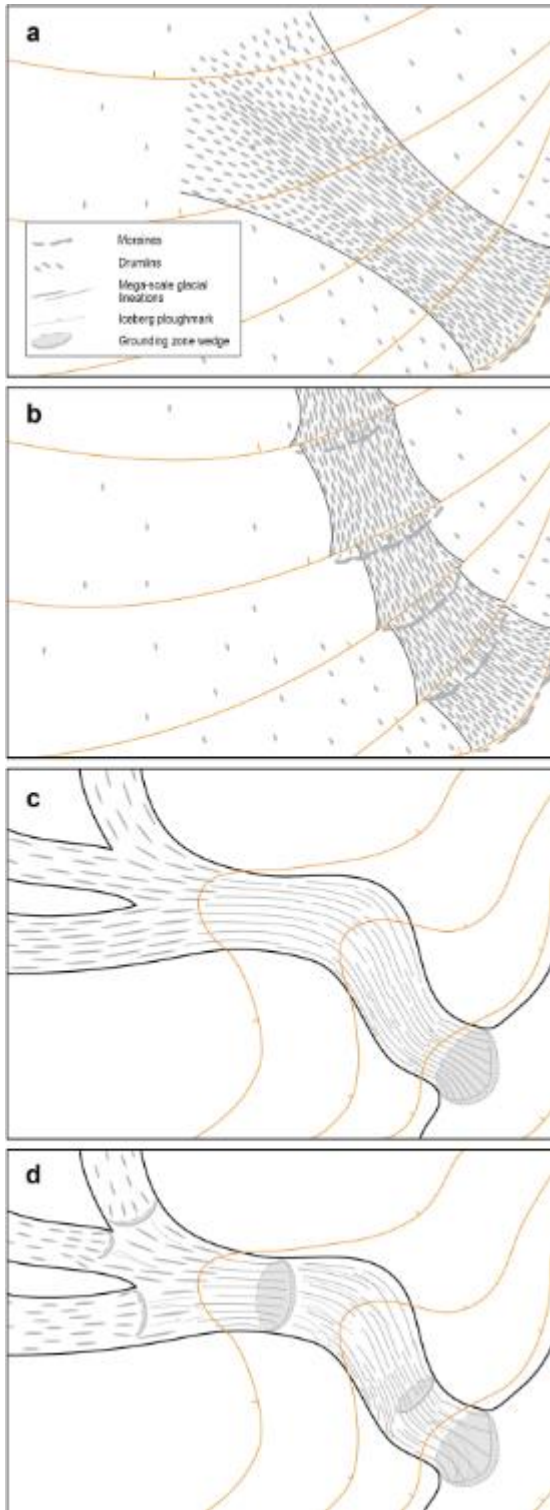
541



542

543 **Extended Data Figure 6: Bathymetric data showing cross-shelf troughs and a well-**
 544 **preserved bedform imprint from a submarine setting. (a)** Cross-shelf troughs formed by
 545 ice streams fed by convergence of ice flow from several fjords along the east coast of Baffin
 546 Island. **(b)** Drumlins and mega-scale glacial lineations on the floor of Eclipse Sound
 547 (location shown in (a)). High resolution swath bathymetry data in (a) from IBCAO⁵⁶ and in
 548 (b and c) from IBCAO⁵⁶ and ArcticNet⁵⁷. Figure redrawn from Margold et al. (2015)⁴⁸.

549

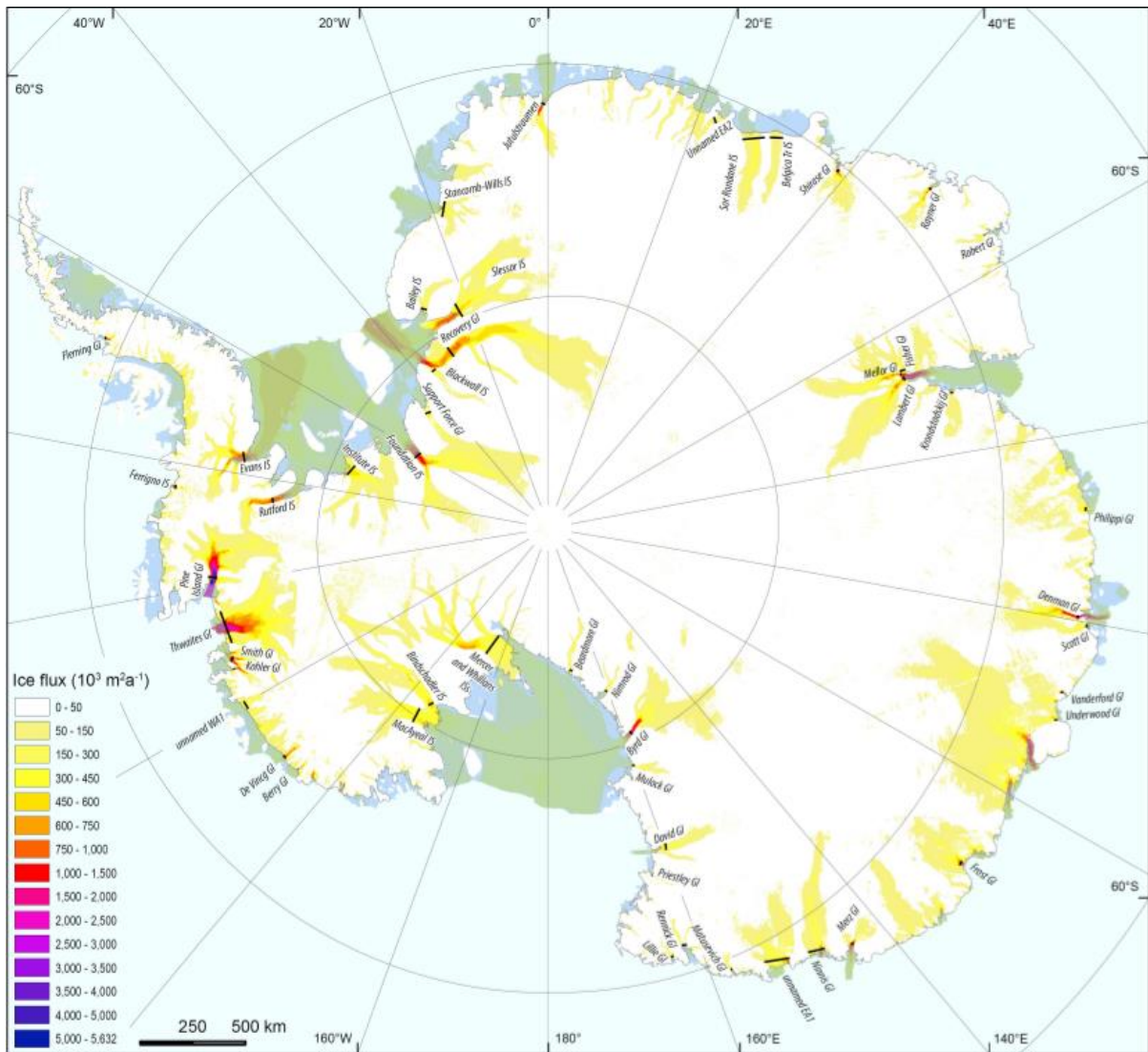


550

551 **Extended Data Figure 7: Schematic demonstrating the method used to bracket the age**
 552 **of the spatial footprint of palaeo-ice streams in both terrestrial and marine settings.**

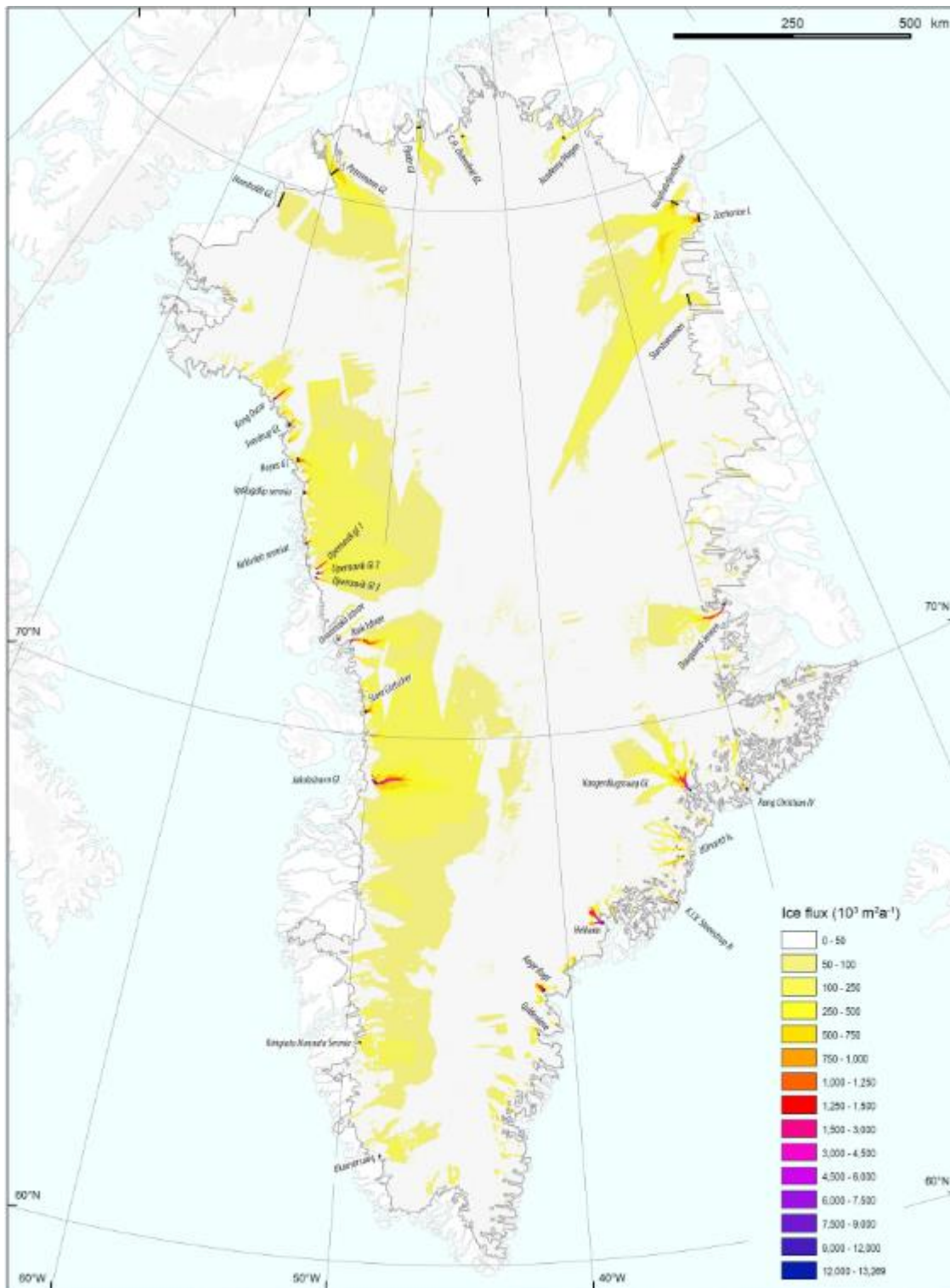
553 These methods have been used extensively in previous work, but usually on small samples of
 554 ice streams (e.g. refs ^{20,21, 36, 37, 42,43}). In some cases, terrestrial ice streams are active, but then
 555 deactivate (shutdown) as the ice margin retreats (a), enabling them to be bracketed between a
 556 small number of dated ice margins and implying a short duration of operation. In other cases,
 557 ice streams remain active during deglaciation and continually remould their landform

558 assemblage, leaving a more complicated time-integrated landform record, often with a series
559 of overprinted landforms **(b)**, and implying a longer duration of operation. The same
560 scenarios are shown for a topographically-controlled marine-terminating ice stream in **(c)** and
561 **(d)**.
562



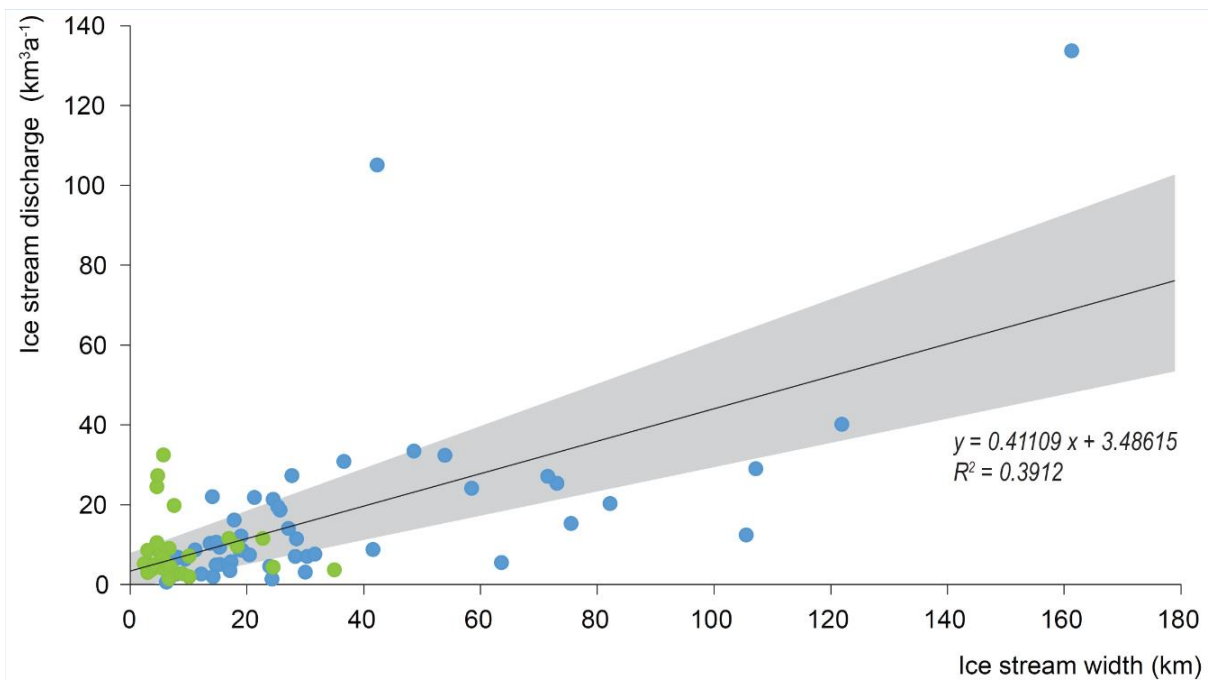
563

564 **Extended Data Figure 8: Location of ice streams in Antarctica where discharge was**
 565 **estimated from existing datasets of velocity⁴⁵, grounding line position⁴⁶ and ice**
 566 **thickness³⁰. Regression analysis reveals a weak relationship between their width and**
 567 **discharge (Extended Data Figure 10), which we use to estimate the discharge of palaeo-ice**
 568 **streams where we only know their width (see Methods)**
 569



570

571 **Extended Data Figure 9: Location of ice streams in Greenland where discharge was**
 572 **estimated from existing datasets of velocity⁴⁴, grounding line position⁴⁴ and ice**
 573 **thickness²⁹. Regression analysis reveals a weak relationship between their width and**
 574 **discharge (Extended Data Figure 10), which we use to estimate the discharge of palaeo-ice**
 575 **streams where we only know their width (see Methods)**
 576



577

578

579 **Extended Data Figure 10: Relationship between ice stream discharge and width for 81**
 580 **active ice streams in Antarctica and Greenland.** Discharge calculations derived from
 581 velocity data in 2008-2009 (Greenland: green dots)⁴⁴ and 2007-2009 (Antarctica: blue dots)⁴⁶.
 582 Grey shading shows the 95% confidence intervals of the linear regression. Measured ice
 583 stream locations are shown in [Extended Data Figure's 8 and 9](#).

584

585

586 **Extended Data References:**

587

- 588 47. Global Digital Elevation Model (GTOPO30), U.S. Geological Survey, EROS Data Center
 589 Distributed Active Archive Center (EDC DAAC). Edition 2004.
- 590 48. Margold, M., Stokes, C.R. & Clark, C.D. Ice streams in the Laurentide Ice Sheet:
 591 identification, characteristics and comparison to modern ice sheets. *Earth-Science*
 592 *Reviews* **143**, 117-146 (2015).
- 593 49. Briner, J.P., Miller, G.H., Davis, P.T. & Finkel, R.C. Cosmogenic radionuclides from
 594 fjord landscapes support differential erosion by overriding ice sheets. *Geol. Soc. Am. Bull.*
 595 **118** (3-4), 406-420 (2006).
- 596 50. Shaw, J. et al., A conceptual model of the deglaciation of Atlantic Canada. *Quat. Sci. Rev.*
 597 **19** (10), 959-980 (2006).
- 598 51. Kleman, J. et al., North American Ice Sheet build-up during the last glacial cycle, 115-21
 599 kyr. *Quat. Sci. Rev.* **29** (17-18), 2036-2051 (2010).
- 600 52. Lakeman, T.R., & England, J.H. Palaeo-glaciological insights from the age and
 601 morphology of the Jesse moraine belt, western Canadian Arctic. *Quat. Sci. Rev.* **47**, 82-
 602 100 (2012).
- 603 53. Lakeman, T.R., & England, J.H. Late Wisconsinan glaciation and postglacial relative sea-
 604 level change on western Banks Island, Canadian Arctic Archipelago. *Quat. Sci. Rev.* **80**
 605 (1), 99-112 (2013).
- 606 54. Jakobsson, M. et al., Arctic Ocean glacial history. *Quat. Sci. Rev.* **92**, 40-67 (2014).

- 607 55. Nixon, F.C. & England, J.H. Expanded Late Wisconsinan ice cap and ice sheet margins in
608 the western Queen Elizabeth Islands, Arctic Canada. *Quat. Sci. Rev.* **91**, 146-164 (2014).
- 609 56. Jakobsson, M. et al., The International Bathymetric Chart of the Arctic Ocean (IBCAO)
610 Version 3.0. *Geophys. Res. Lett.*, doi: 10.1029/2012GL052219 (2012).
- 611 57. ArcticNet, 2013: <http://www.omg.unb.ca/Projects/Arctic/> [accessed 1st December 2013]
612
613